International Scholarly Research Network
ISRN Optics
Volume 2012, Article ID 193185, 7 pages
doi:10.5402/2012/193185

Research Article

Effect of Stepwise Replacement of LiF by Bi_2O_3 and of Annealing on Optical Properties of $LiF \cdot B_2O_3$ Glasses

Susheel Arora,[1] Virender Kundu,[2] D. R. Goyal,[1] and A. S. Maan[1]

[1] *Department of Physics, Maharshi Dayanand University, Rohtak 124 001, India*
[2] *Department of Electronic Science, Kurukshetra University, Kurukshetra 136 119, India*

Correspondence should be addressed to Susheel Arora, susheel_arora@yahoo.com

Received 29 December 2011; Accepted 29 January 2012

Academic Editors: M. Farries, L. R. P. Kassab, and Y. Tsuji

Bismuth fluoroborate glasses with compositions $x Bi_2O_3 \cdot (40 - x)LiF \cdot 60\ B_2O_3$ ($x = 0, 5, 10, 15,$ and 20) are synthesized by melt-quench method. Optical characterization was carried out to examine variation of optical band gap energy (E_g) and Urbach energy (E_U) with respect to the concentration. It reflects the effect of stepwise replacement of non-oxide and less polarizable LiF by an oxide and more polarizable (Bi_2O_3) group on the optical properties of the samples. The value of E_g decreases with increase in concentration of Bi_2O_3. The samples were subjected to annealing at different temperatures (300°C, 350°C, and 400°C), and the effect of annealing on the optical properties of various samples was again studied. Annealing affects remarkably the values of E_g and E_U in the samples with $x = 0$.

1. Introduction

Fast cooling of the molten form of a substance makes it difficult to form a crystalline phase. Instead, it forms the amorphous phase of the substance. Glassy nature of the substance, philosophically, is just the lack of time required for the atoms or molecules to form a long range order. The sheet-like structure of boron-oxygen triangles in borate glasses, with their ability to connect themselves to form a network, has popularized B_2O_3 as one of the best glass former [1, 2]. The glass formation demands a random arrangement of various atomic and molecular species which easily form in borate glasses. A number of modifications in the properties of the borate glasses, with the addition of alkali halides, have been reported so far [3–9]. The inclusion of LiF in the borate glass network brings out some structural changes [3], which in turn become responsible for the change in various properties. Some oxygen atoms get replaced by fluorine ions in the network to form new units like BO_2F, BO_2F_2, BOF_3, and BO_3F [4–6]. Also, there may be an increase in the number of polyhedral groups of boron and oxygen, which in turn increases the number of nonbridging oxygen atoms [7–9]. Because of high third-order nonlinear optical susceptibility of Bi_2O_3, caused by high density and refractive index [10, 11], it has numerous nonlinearity applications such as optical switching [12, 13], supercontinuum generation [14], wavelength conversion [15], and so forth. Also, bismuth ion acts as an efficient luminescent activator with applications in lasers as a sensitizer for some rare earth ions [16, 17].

Various properties like optical, physical, electrical, and structural, and so forth are always sensitive to the variations in the microstructure of the substance. Due to nonhomogeneous cooling of the melt, the structure and, therefore, optical behavior of the material are affected. B_2O_3 glasses change their characteristics remarkably, when subjected to different annealing temperatures [18–22]. In these glasses, it is never discouraged to expect the formation of B_3O_6 rings called boroxol rings, by the combination of BO_3 groups. Raman spectroscopy reveals that for annealing temperature greater than the glass transition temperature, the concentration of boroxol rings increases with decrease in temperature [21]. There appears a residual stress in such materials. During annealing of a glass, a thermodynamical and mechanical steady state is achieved after a specific time and temperature.

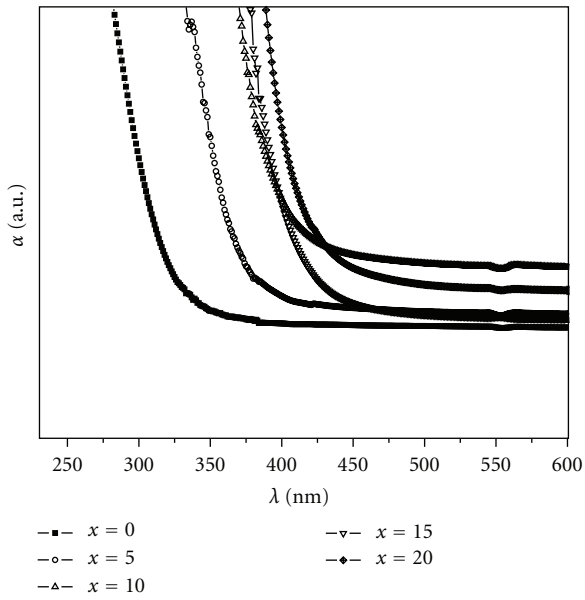

Figure 1: Optical absorption coefficient versus wavelength plots for samples as prepared with $x = 0, 5, 10, 15$, and 20 in the compositions $x\mathrm{Bi_2O_3}\cdot(40 - x)\mathrm{LiF}\cdot 60\ \mathrm{B_2O_3}$.

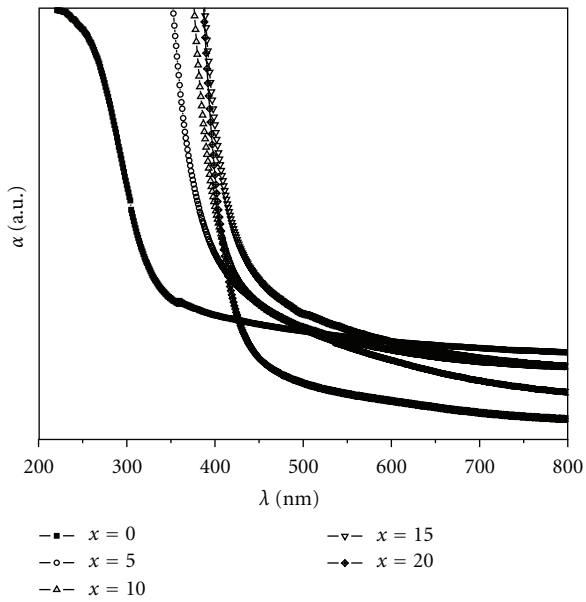

Figure 2: Optical absorption coefficient versus wavelength plots for samples annealed at 300°C with $x = 0, 5, 10, 15$, and 20 in the compositions $x\mathrm{Bi_2O_3}\cdot(40 - x)\mathrm{LiF}\cdot 60\ \mathrm{B_2O_3}$.

The purpose of this paper is to report the change in optical properties of $\mathrm{LiF}\cdot\mathrm{B_2O_3}$ glasses with the stepwise replacement of LiF by $\mathrm{Bi_2O_3}$. The addition of $\mathrm{Bi_2O_3}$ provides an opportunity for the new molecular units to be formed with more number of NBOs. It also affects the overall polarizability of the glass network. Both of these factors result in a change in optical band gap energy.

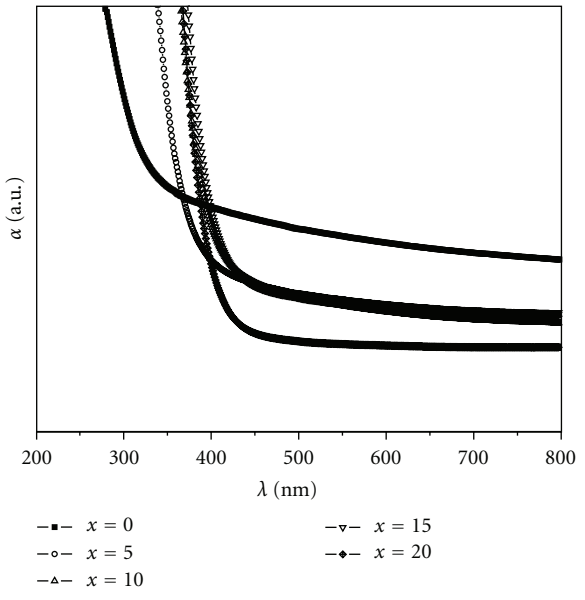

Figure 3: Optical absorption coefficient versus wavelength plots for samples annealed at 350°C with $x = 0, 5, 10, 15$, and 20 in the compositions $x\mathrm{Bi_2O_3}\cdot(40 - x)\mathrm{LiF}\cdot 60\ \mathrm{B_2O_3}$.

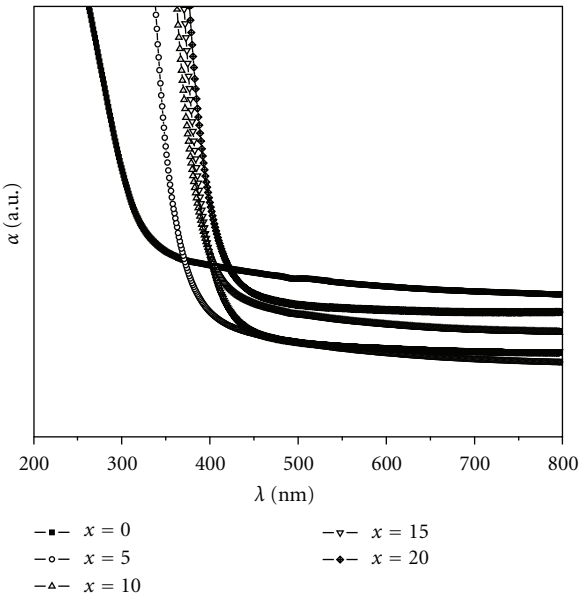

Figure 4: Optical absorption coefficient versus wavelength plots for samples annealed at 400°C with $x = 0, 5, 10, 15$, and 20 in the compositions $x\mathrm{Bi_2O_3}\cdot(40 - x)\mathrm{LiF}\cdot 60\ \mathrm{B_2O_3}$.

2. Experimental Details

2.1. Sample Preparation. $\mathrm{Bi_2O_3}$ containing fluoroborate glasses with compositions $x\mathrm{Bi_2O_3}\cdot(40\text{-}x)\mathrm{LiF}\cdot 60\ \mathrm{B_2O_3}$ ($x = 0, 5, 10, 15$ and 20) glasses were synthesized through melt-quench method using $\mathrm{Bi_2O_3}$, LiF, and $\mathrm{H_3BO_3}$, reagent grade powders. Various powdered materials were taken in grams equal to their molecular masses and then were mixed uniformly according to their percentage presence in various

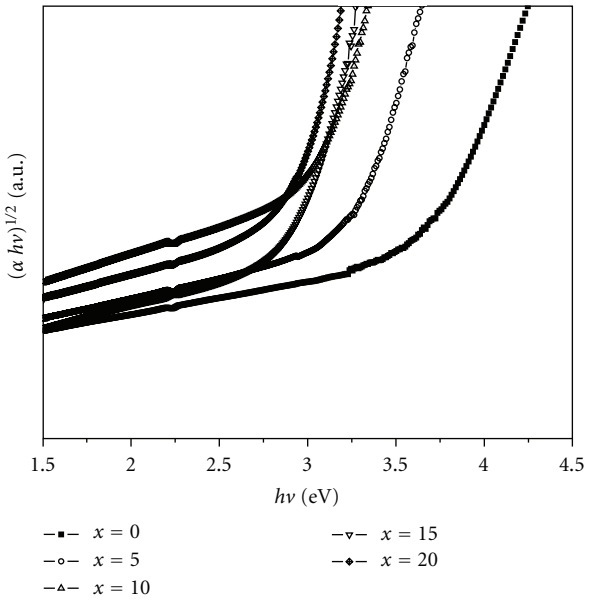

Figure 5: Tauc's plots with $r = 2$ for samples as prepared with $x = 0, 5, 10, 15$, and 20 in the compositions $x\mathrm{Bi_2O_3}\cdot(40 - x)\mathrm{LiF}\cdot 60\ \mathrm{B_2O_3}$.

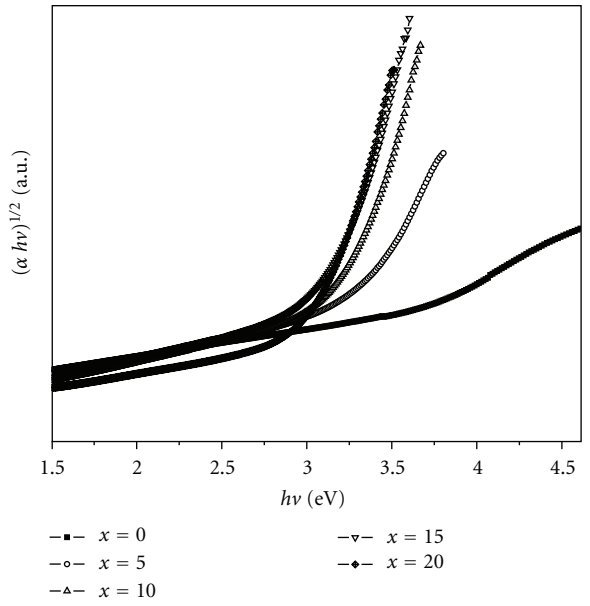

Figure 6: Tauc's plots with $r = 2$ for samples annealed at 300°C with $x = 0, 5, 10, 15$, and 20 in the compositions $x\mathrm{Bi_2O_3}\cdot(40 - x)\mathrm{LiF}\cdot 60\ \mathrm{B_2O_3}$.

samples. The uniform mixture was heated at 1273 K for 30 minutes. The bubble free-melt formed was pressed between two carbon plates at room temperature. The glassy samples were thus obtained in form of thin pallets with an average thickness of 1 mm each.

2.2. Optical Characterization. Optical characterization was carried out using Perkin-Elmer UV-Visible spectrophotometer in the range 200–1000 nm at room temperature. A plot between the absorption and wavelength of incident radiations is obtained for further analysis.

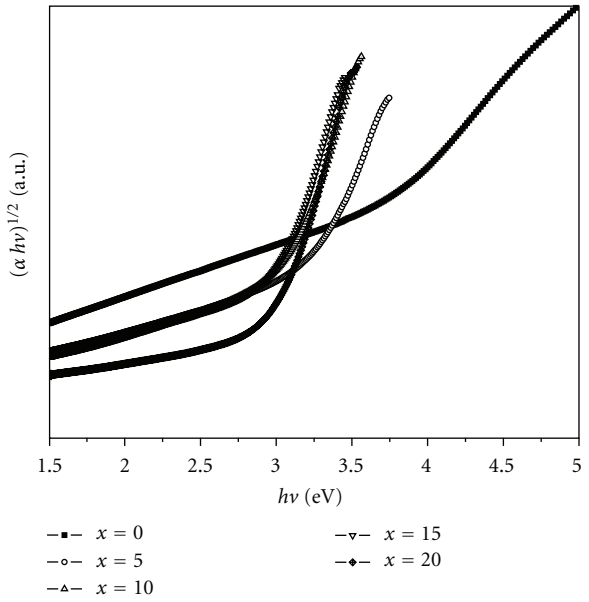

Figure 7: Tauc's plots with $r = 2$ for samples annealed at 350°C with $x = 0, 5, 10, 15$, and 20 in the compositions $x\mathrm{Bi_2O_3}\cdot(40 - x)\mathrm{LiF}\cdot 60\ \mathrm{B_2O_3}$.

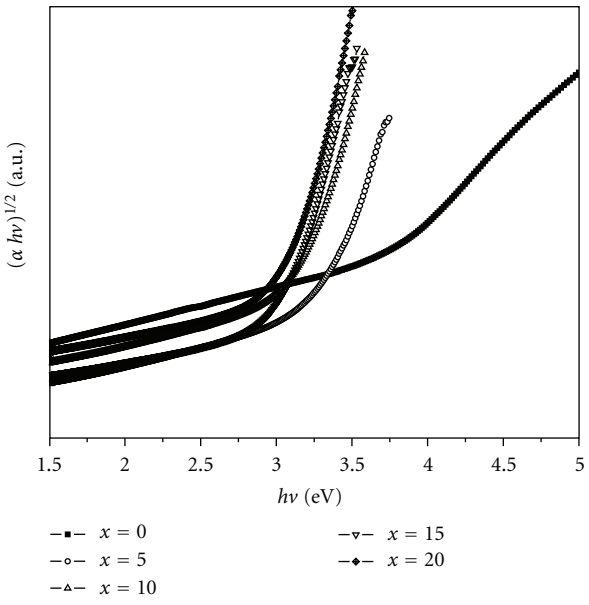

Figure 8: Tauc's plots with $r = 2$ for samples annealed at 400°C with $x = 0, 5, 10, 15$, and 20 in the compositions $x\mathrm{Bi_2O_3}\cdot(40 - x)\mathrm{LiF}\cdot 60\ \mathrm{B_2O_3}$.

2.3. Annealing. Samples were annealed at 300°C, 350°C, and 400°C for 2 hrs each. The samples so obtained were again tested for optical and physical properties.

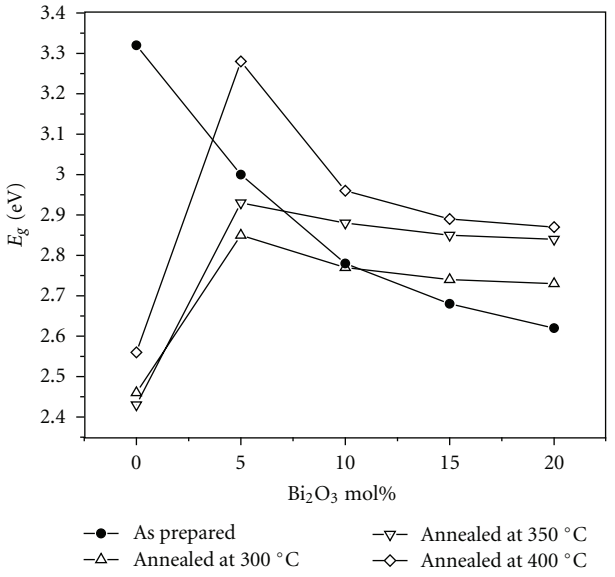

Figure 9: Variation of E_g with composition for samples with x = 0, 5, 10, 15, and 20 in the compositions $x\mathrm{Bi_2O_3}\cdot(40 - x)\mathrm{LiF}\cdot 60\ \mathrm{B_2O_3}$.

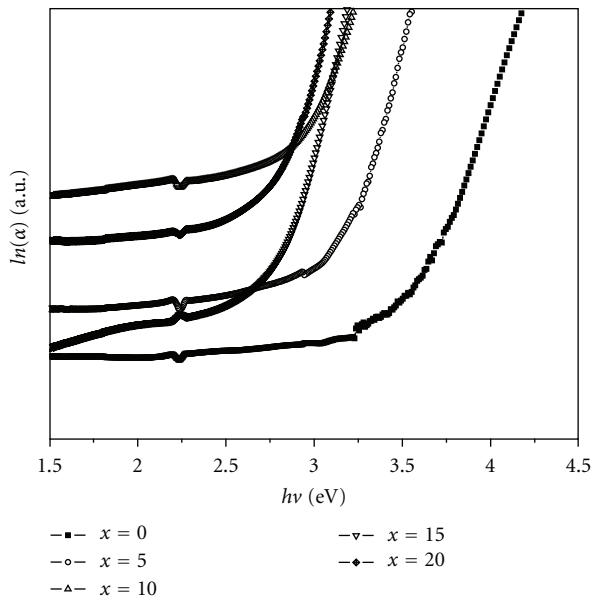

Figure 10: Urbach plots for samples as prepared with x = 0, 5, 10, 15, and 20 in the compositions $x\mathrm{Bi_2O_3}\cdot(40 - x)\mathrm{LiF}\cdot 60\ \mathrm{B_2O_3}$.

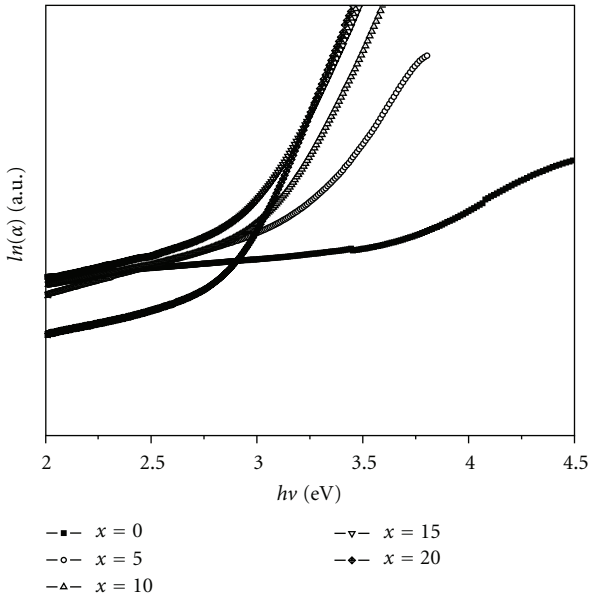

Figure 11: Urbach plots for samples annealed at 300°C with x = 0, 5, 10, 15, and 20 in the compositions $x\mathrm{Bi_2O_3}\cdot(40 - x)\mathrm{LiF}\cdot 60\ \mathrm{B_2O_3}$.

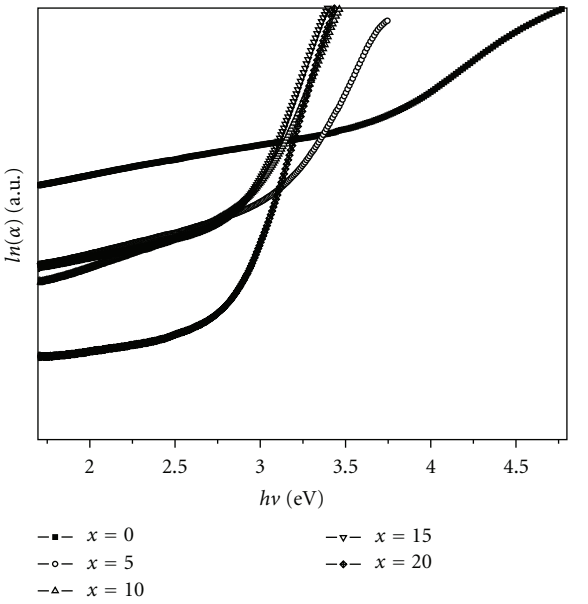

Figure 12: Urbach plots for samples annealed at 350°C with x = 0, 5, 10, 15, and 20 in the compositions $x\mathrm{Bi_2O_3}\cdot(40 - x)\mathrm{LiF}\cdot 60\ \mathrm{B_2O_3}$.

3. Results and Discussion

3.1. Optical Analysis. A series of samples in $x\mathrm{Bi_2O_3}\cdot(40 - x)\mathrm{LiF}\cdot 60\ \mathrm{B_2O_3}$ compositions with x = 0, 5, 10, 15, and 20 were tested for UV-visible absorption at room temperature. The absorption profiles of as-prepared and annealed samples are depicted in Figures 1, 2, 3, and 4, which contain plots of absorption coefficient $\alpha(\nu)$ versus wavelength.

The absorption coefficient $\alpha(\nu)$ is formulated in terms of transmitted intensity (I_t), incident intensity (I_i), and the thickness of the sample (t) [23] and is given as

$$\alpha(\nu) = \left(\frac{1}{t}\right)\ln\left(\frac{I_i}{I_t}\right). \quad (1)$$

From Figures 1, 2, 3, and 4, one can observe that there is an absence of sharp absorption edge in all the plots. This

Table 1: Cutoff wavelength (λ_{cutoff}), optical band gap energy E_g and Urbach energy (E_U) for the samples with $x = 0, 5, 10, 15$, and 20 in the compositions $x\mathrm{Bi_2O_3}\cdot(40 - x)\mathrm{LiF}\cdot 60\ \mathrm{B_2O_3}$.

	x (mol%)	λ_{cutoff} (nm)	E_g (eV)	B (cm eV)$^{-1}$	E_U (eV)
As Prepared	0	334	3.32	1.614	0.510
	5	384	3.00	1.868	0.231
	10	408	2.78	1.932	0.213
	15	433	2.68	2.003	0.213
	20	442	2.62	2.095	0.194
Annealed at 300°C	0	377	2.46	1.073	1.376
	5	394	2.85	1.614	0.499
	10	410	2.77	1.868	0.404
	15	413	2.74	1.932	0.364
	20	416	2.73	2.003	0.296
Annealed at 350°C	0	361	2.43	0.745	1.842
	5	400	2.93	1.432	0.649
	10	419	2.88	1.868	0.488
	15	432	2.85	2.003	0.456
	20	426	2.84	2.081	0.404
Annealed at 400°C	0	361	2.56	1.036	1.428
	5	377	3.28	1.809	0.384
	10	413	2.96	2.003	0.404
	15	416	2.89	2.081	0.344
	20	423	2.87	2.268	0.364

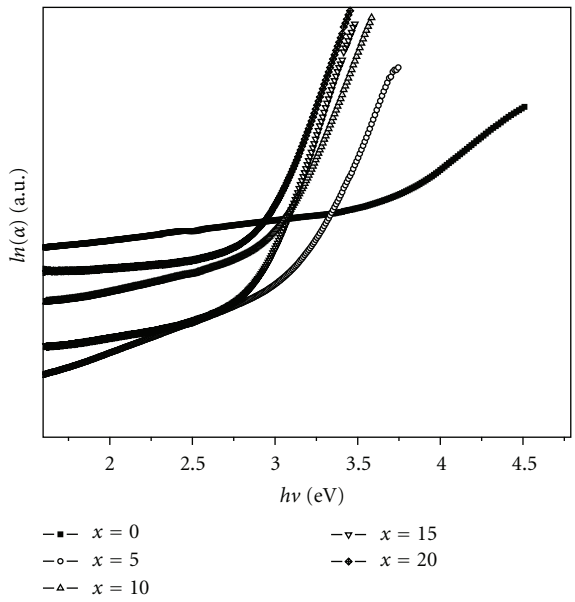

Figure 13: Urbach plots for samples annealed at 400°C with $x = 0$, 5, 10, 15, and 20 in the compositions $x\mathrm{Bi_2O_3}\cdot(40 - x)\mathrm{LiF}\cdot 60\ \mathrm{B_2O_3}$.

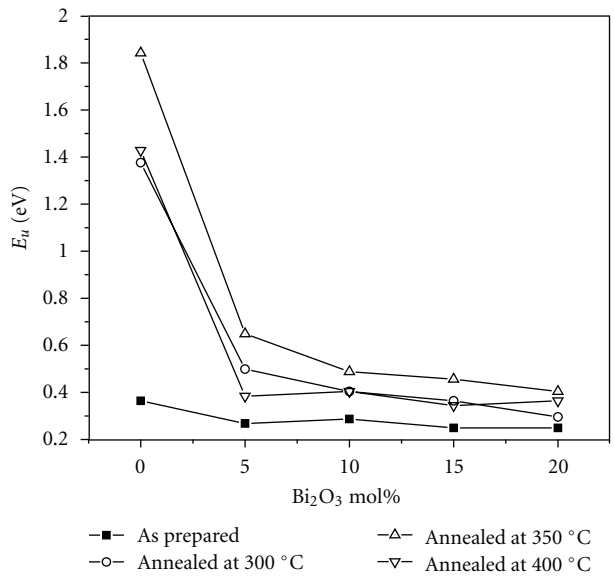

Figure 14: Variation of Urbach tail energy with composition for samples with $x = 0$, 5, 10, 15, and 20 in the compositions $x\mathrm{Bi_2O_3}\cdot(40 - x)\mathrm{LiF}\cdot 60\ \mathrm{B_2O_3}$.

confirms that the samples are amorphous in nature. Calculation of optical band gap energy explores the optical behavior of a sample in terms of its transparency towards electromagnetic radiations. The optical band gap energy (E_g) is related to the absorption coefficient $\alpha(\nu)$ [23] as

$$\alpha h\nu = \mathrm{B}\left(h\nu - E_g\right)^r. \quad (2)$$

In this equation, ν is the frequency of incident radiation and B is a constant named as band tailing parameter. Value of the index r suggests the nature of transitions taking place in the sample. For indirect allowed and forbidden transitions $r = 2$ and 3, respectively, and for direct allowed and forbidden transitions r equals 1/2 and 2/3, respectively. Tauc's plots $[(\alpha h\nu)^{1/r}$ versus $h\nu$, $r = 2]$ for the reported samples are shown in Figures 5, 6, 7 and 8. The values of optical band gap

energy E_g are obtained by extrapolating the linear regions of tauc's plots. The variation of E_g for as-prepared and annealed samples against composition is listed in Table 1 and plotted in Figure 9.

There is a continuous decrease in the optical band gap energy starting from $x = 0$ to $x = 20$. In glassy materials, the decrease in optical band gap energy is often attributed to the increase in polarizability. Also in oxide glasses, it is supported by the increase in disorder due to increase in number of nonbridging oxygen atoms (NBOs). In case of presently reported samples, there is an increase in the polarizability as concentration of LiF, whose polarizability is less, is replaced stepwise by concentration of more polarizable Bi_2O_3. Also there is quite a good scope of increase in the number of NBOs, as there is a replacement of a non-oxide group (LiF) taking place by an oxide group (Bi_2O_3) from $x = 0$ to $x = 20$.

Interestingly, annealing at different temperatures has remarkably affected E_g for the sample with no Bi_2O_3 added. For samples with $x = 5$ also, it first decreases for annealing temperature 300°C and the increases for higher temperatures. E_g increases with annealing temperature, in general, for all other concentrations. In samples with $x = 0$, it is expected that annealing causes BO_4 units to be transformed into BO_3^- units, which have one NBO each. Therefore, E_g decreases on account of increasing no. of NBOs. In samples other than $x = 0$, annealing causes more BO_3 groups to connect themselves to form boroxol rings and to decrease the no. of NBOs. For $x = 5$, the formation of boroxol rings overshoots the formation of BO_3^- units at 400°C. Although the trend of variation of E_g in annealed samples remains almost same with respect to concentration as it is in the as-prepared samples.

In the low absorption region of tauc's plot, the absorption coefficient is related to photon energy [24] as

$$\alpha \sim \exp\left(\frac{h\nu}{E_U}\right). \quad (3)$$

In this equation E_U is named as urbach tail energy which corresponds to the width of the tail states in the mobility gap. E_U arises due to presence of the disordered arrangement of atoms, which causes the mobility edges to enter in the mobility gap and give rise to the tail states. Formation of such localized states can thus be attributed to the random potential fluctuations [25]. Generally, in such states the phonon-assisted electronic transitions take place [26, 27]. The formation of such states in the materials makes it the indirect band gap material. Therefore, one can conclude that the reported samples are the indirect band gap materials.

The value of E_U for the reported samples is calculated from the inverse of the slopes of the linear parts of the Urbach plots ($\ln \alpha$ v/s $h\nu$), shown in Figures 10, 11, 12, and 13. The values of E_U for as-prepared and annealed samples are listed in Table 1, and the variation of E_U is plotted against the composition in Figure 14.

Value of E_U remains almost same for all as-prepared samples but increases remarkably for $x = 0$ when annealed at different temperatures. The reason is the same as given for decrease in band gap energy that is, conversion of BO_4 units to BO_3^- units, thereby increasing the no. of NBOs and hence disorder. For other samples, E_U increases due to annealing, keeping the trend of variation similar with respect to the concentration.

4. Conclusions

(1) Optical band gap energy in the series of samples $x\mathrm{Bi_2O_3}\cdot(40 - x)\mathrm{LiF}\cdot 60\ \mathrm{B_2O_3}$ decreases from $x = 0$ to $x = 20$ due to increased polarizability and no. of NBOs in the samples.

(2) Annealing at different temperatures decreases the value of E_g for $x = 0$ due to conversion of BO_4 units into BO_3^- units, thereby increasing the no. of NBOs. For samples with $x = 5$ also, annealing at 300°C firstly causes E_g to decrease but it increases for increase in annealing temperature. This is because with increase in annealing temperature, formation of boroxol rings dominates over formation of BO_3^- units, hence decreasing NBOs. For other samples, E_g the increases with annealing temperature, again due to increase in NBOs.

(3) In case of as-prepared samples, Urbach energy varies slightly with concentration with maximum for $x = 0$.

(4) For same reasons explained above, after annealing, E_U is affected appreciably for $x = 0$ and $x = 5$. For other samples, it is slightly increased keeping the trend of variation similar.

References

[1] C. Boussard-Plédel, M. Le Floch, G. Fonteneau et al., "The structure of a boron oxyfluoride glass, an inorganic cross-linked chain polymer," *Journal of Non-Crystalline Solids*, vol. 209, no. 3, pp. 247–256, 1997.

[2] G. D. Chryssikos, M. S. Bitsis, J. A. Kapoutsis, and E. I. Kamitsos, "Vibrational investigation of lithium metaborate-metaaluminate glasses and crystals," *Journal of Non-Crystalline Solids*, vol. 217, no. 2-3, pp. 278–290, 1997.

[3] C. Boussard-Plédel, G. Fonteneau, and J. Lucas, "Boron oxyfluoride glasses in the BOF system: new polymeric spaghetti-type glasses," *Journal of Non-Crystalline Solids*, vol. 188, no. 1-2, pp. 147–152, 1995.

[4] N. Soga, "Elastic moduli and fracture toughness of glass," *Journal of Non-Crystalline Solids*, vol. 73, no. 1–3, pp. 305–313, 1985.

[5] I. Z. Hager, "Elastic moduli of boron oxyfluoride glasses: experimental determinations and application of Makishima and Mackenzie's theory," *Journal of Materials Science*, vol. 37, no. 7, pp. 1309–1313, 2002.

[6] I. Z. Hager and M. El-Hofy, "Investigation of spectral absorption and elastic moduli of lithium haloborate glasses," *Physica Status Solidi (A)*, vol. 198, no. 1, pp. 7–17, 2003.

[7] J. E. Shelby and L. K. Downie, "Properties and structure of sodium fluoroborate glasses," *Physics and Chemistry of Glasses*, vol. 30, no. 4, pp. 151–154, 1989.

[8] G. D. Chryssikos, E. I. Kamitsos, A. P. Patsis, M. S. Bitsis, and M. A. Karakassides, "The devitrification of lithium metaborate: polymorphism and glass formation," *Journal of Non-Crystalline Solids*, vol. 126, no. 1-2, pp. 42–51, 1990.

[9] E. I. Kamitsos, A. P. Patsis, and G. D. Chryssikos, "Infrared reflectance investigation of alkali diborate glasses," *Journal of Non-Crystalline Solids*, vol. 152, no. 2-3, pp. 246–257, 1993.

[10] C. Hwang, S. Fujino, and K. Morinaga, "Density of Bi_2O_3-B_2O_3 binary melts," *Journal of the American Ceramic Society*, vol. 87, no. 9, pp. 1677–1682, 2004.

[11] I. I. Oprea, H. Hesse, and K. Betzler, "Optical properties of bismuth borate glasses," *Optical Materials*, vol. 26, no. 3, pp. 235–237, 2004.

[12] S. Fujiwara, T. Suzuki, N. Sugimoto, H. Kanbara, and K. Hirao, "THz optical switching in glasses containing bismuth oxide," *Journal of Non-Crystalline Solids*, vol. 259, no. 1-3, pp. 116–120, 1999.

[13] N. Sugimoto, "Ultrafast optical switches and wavelength division multiplexing (WDM) amplifiers based on bismuth oxide glasses," *Journal of the American Ceramic Society*, vol. 85, no. 5, pp. 1083–1088, 2002.

[14] G. Brambilla, F. Koizumi, V. Finazzi, and D. J. Richardson, "Supercontinuum generation in tapered bismuth silicate fibres," *Electronics Letters*, vol. 41, no. 14, pp. 795–797, 2005.

[15] J. H. Lee, K. Kikuchi, T. Nagashima, T. Hasegawa, S. Ohara, and N. Sugimoto, "All fiber-based 160-Gbit/s add/drop multiplexer incorporating a 1-m-long Bismuth Oxide-based ultra-high nonlinearity fiber," *Optics Express*, vol. 13, no. 18, pp. 6864–6869, 2005.

[16] C. H. Kim, H. L. Park, and S. I. Mho, "Photoluminescence of Eu^{3+} and Bi^{3+} IN $Na_3YSi_3O_9$," *Solid State Communications*, vol. 101, no. 2, pp. 109–113, 1997.

[17] A. M. Srivastava, "Luminescence of divalent bismuth in M^{2+} BPO_5 (M^{2+} = Ba^{2+}, Sr^{2+} and Ca^{2+})," *Journal of Luminescence*, vol. 78, no. 4, pp. 239–243, 1998.

[18] C. Martin, C. Chaumont, J. P. Sanchez, and J. C. Bernier, "Influence of preparation process on physical properties and devitrification of $Li_2B_2O_4$ (0,9) $LiFe_5O_8$ (0,1) glasses," *Journal de Physique Colloques*, vol. 46, no. C8, pp. 585–589, 1985.

[19] A. M. Harold, "Variations of refractive index of glass with time and temperature in annealing region," *Journal of the American Ceramic Society*, vol. 28, no. 1, p. 1, 1945.

[20] W. T. Leroy, W. R. Fred, and T. B. Florence, "Refractive uniformity of a borosilicate glass after different annealing treatments," *Journal of Research of the National Bureau of Standards*, vol. 49, no. 1, pp. 21–32, 1952.

[21] N. V. Surovtsev, J. Wiedersich, A. E. Batalov, V. N. Novikov, M. A. Ramos, and E. Rössler, "Inelastic light scattering in B_2O_3 glasses with different thermal histories," *Journal of Chemical Physics*, vol. 113, no. 14, pp. 5891–5900, 2000.

[22] S. A. Kartha, M. A. Ittyachen, B. Pradeep, and M. Abdul Khadar, "Effect of annealing on the optical properties of B_2O_3-Li_2O-PbO glass thin films," *Journal of Materials Science Letters*, vol. 22, no. 1, pp. 9–11, 2003.

[23] E. A. Devis and N. F. Mott, "Conduction in non-crystalline systems V. Conductivity, optical absorption and photoconductivity in amorphous emiconductors," *Philosophical Magazine*, vol. 22, pp. 0903–0922, 1970.

[24] F. Urbach, "The long-wavelength edge of photographic sensitivity and of the electronic Absorption of Solids," *Physical Review*, vol. 92, no. 5, p. 1324, 1953.

[25] A. A. Kutub, A. E. Mohamed-Osman, and C. A. Hogarth, "Some studies of the optical properties of copper phosphate glasses containing praseodymium," *Journal of Materials Science*, vol. 21, no. 10, pp. 3517–3520, 1986.

[26] C. Dayanand, G. Bhikshamaiah, and M. Salagram, "IR and optical properties of PbO glass containing a small amount of silica," *Materials Letters*, vol. 23, no. 4–6, pp. 309–315, 1995.

[27] K. L. Chopra and S. K. Bahl, "Exponential tail of the optical absorption edge of amorphous semiconductors," *Thin Solid Films*, vol. 11, no. 2, pp. 377–388, 1972.